A NON-DESTRUCTIVE PROFILE MONITOR FOR HIGH INTENSITY BEAMS

W. Blokland and S. Cousineau, ORNL*, Oak Ridge, TN 37831, U.S.A

Abstract

A non-destructive profile monitor has been installed and commissioned in the accumulator ring of Spallation Neutron Source (SNS). The SNS Ring accumulates during a 1 ms cycle high intensity proton bunches of up to 1.5e14 protons with a typical peak current of over 50 A and a bunch length of about 0.7 μs.

The profile monitor consists of two systems, one for each plane, with electron guns, correctors, deflectors, and quadrupole magnets to produce pulsed electron beams that scan through the proton bunch. The electric and magnetic fields of the proton bunch alter the trajectory of the electrons and their projection on a fluorescent screen. The projection is analyzed to determine the transverse profile of the proton bunch. Because the duration of the electron scan is very short compared to the bunch length, the longitudinal profile can be obtained by making multiple scans while varying the time delay relative to the proton bunch.

This paper describes the theory, the hardware and software, analysis, and results of, as well as improvements made to the electron scanners. The results include a comparison of wire scanner profiles of extracted ring beam with the profiles of ring beam from the electron scanner.

INTRODUCTION

The electron scanner measures the transverse profile of a proton beam by analyzing the deflection of electrons by the charged beam's electric field. The effect of the magnetic field has been simulated and was found to have a smaller than 5% effect of the beam profile. This effect mostly manifests itself as a small translation of the electron beam. The electron scanner is a non-destructive alternative to an intercepting profile measurement instrument, such as the wire-scanner, and can be used throughout the neutron production cycle.

By tilting the electron beam, see Fig. 1, the transverse profile can be derived from the angle of deflection of the electrons passing at varying distances from the proton beam center. The derivation is shown in [1] and assumes that the path of the electrons is approximately straight, the net electron energy change over its path is close to zero, and that the effect of the magnetic field of the proton beam can be neglected. The equation describing the electron deflection is:

$$\frac{d\theta}{dx} = \int_L \frac{e}{mv^2} \cdot \frac{\delta(x,y)}{\varepsilon_0} dy$$

where e is the electron charge, m is the electron mass, v is the velocity, $\delta(x,y)$ is the proton beam density distribution, and θ is the electron deflection angle. The formula states that the profile can be reconstructed by taking the derivative of the projected curve.

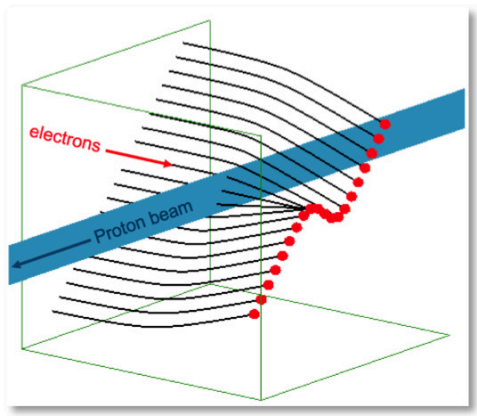

Figure 1: The deflection of a diagonal line of electrons.

While the electrons are similarly deflected if the scan is aligned vertically, one can no longer uniquely associate the electron path with the deflection. One must instead analyze the density distribution of the projected electrons to derive the profile [2], see Fig 2. This method was found, through simulations, to give lower quality results.

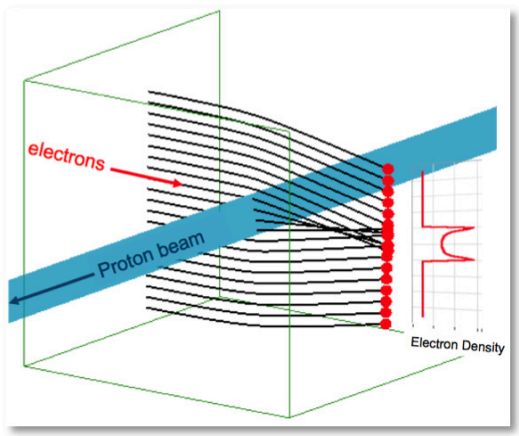

Figure 2: Deflection of a vertical line of electrons and its density distribution when projected on a screen.

* ORNL/SNS is managed by UT-Battelle, LLC, for the U.S. Department of Energy under contract DE-AC05-00OR22725

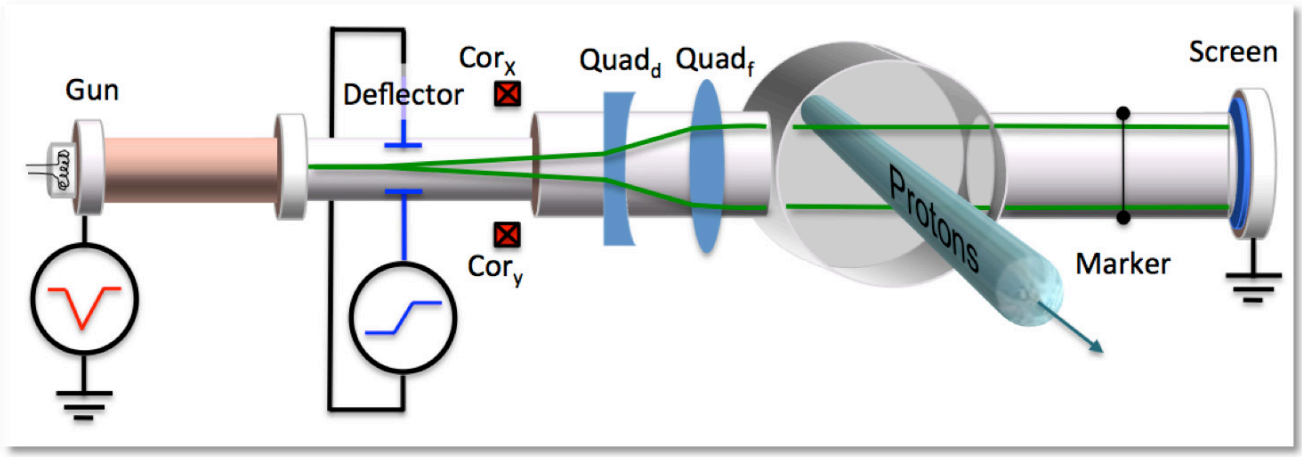

Figure 3: The diagram of the electron scanner.

ELECTRON SCANNER HARDWARE

The electron scanner was built by Budker Institute of Physics based on specifications by SNS. It is designed to produce a much shorter scan of 20 ns compared to the proton bunch length of 630 ns so that the bunch intensity is almost constant during the scan. The shorter scan duration also allows us to slice through the bunch at different times and obtain a longitudinal profile. The layout is shown in Fig. 3 while the installation of both scanners is shown in Fig. 4.

Figure 4: The two electron scanners.

The short scan is produced by a combination of a pulsed electron gun, -60 keV for 1 μs, and a deflector ramping over 20 ns. By pulsing the electron gun, a higher instantaneous current can be generated than with a continuous electron gun, which improves the visibility of the electron curve on the screen. A small aperture reduces the size of the electron beam by scraping most of the beam away. The deflector is oriented at 45 degrees to create a diagonal scan. The width of the scan is expanded by a defocusing quad and then made parallel by a focusing quad. Corrector dipoles allow for a small amount of steering, aligning the electrons through the center of the quads and on the fluorescent screen. Markers placed halfway between the proton beam and the screen are used to verify that the electron beam is parallel to the electron scanner's beam pipe.

Two electron scanners, one for the horizontal and one for the vertical profile, are installed in a straight and low-radiation area of the SNS Ring. Each scanner has a GigE Vision CMOS camera acquiring the images from the fluorescent screen.

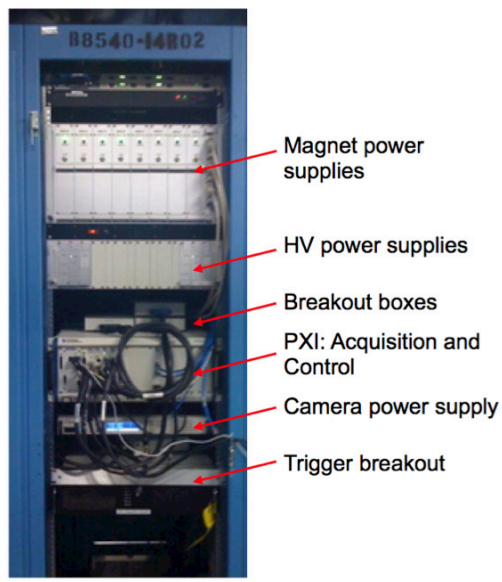

Figure 5: The Electronics for the two scanners.

A PXI-based computer interfaces to all the hardware: the magnets, cameras, power supplies for the electron gun, and the deflectors, see Fig. 5. A custom-made transformer, placed in the tunnel, generates the accelerating voltage from a few hundred volt pulse sent by the High Voltage (HV) power supplies. It also generates the cathode heating current and the deflector voltage.

ELECTRON SCANNER SOFTWARE

A LabVIEW application, see Fig. 6, controls the hardware and acquires the waveforms of the deflectors and HV transformers. The HV waveforms of the transformers are picked up in the tunnel by a copper strip on the transformer's plastic housing. This strip was calibrated by comparing the digitzer waveform to a HV probe waveform, temporarily attached to the electron gun itself.

Default setup files are saved on disk and are read in on startup. The same settings can be used for most of the intensities. For low intensity proton beams, the accelerating voltage is decreased to increase the small deflection of the low charge proton beam and vice versa for high intensity beams. The software can sequence through multiple bunches with the analysis either turned on or off to save the image for off-line analysis.

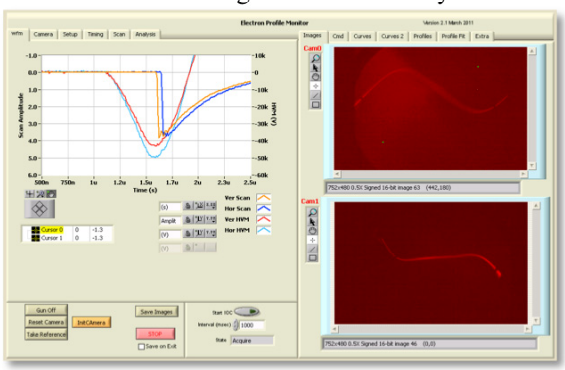

Figure 6: The Electron Scanner application.

Analysis

The image of a typical scan for the horizontal profile with proton beam present is shown in Figure 7. Note the cutouts in the curve caused by the markers. These markers are used to verify the parallelism of the electron trajectories. To calculate the profile from this curve, the derivative, *dy/dx*, must be taken.

The image is first processed with a lowpass filter and a smoothing kernel to remove specs from the image. The specs are temporary and often due to radiation hitting the camera but can confuse the analysis. Optionally, a background image can be subtracted.

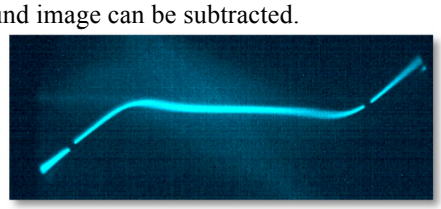

Figure 7: Electron projection for the horizontal profile affected by the proton beam.

The next step is to find the peak for each column in the image. At times electrons from outside the intended scan make it to the screen and form a blob on the screen, therefore only those peaks close to a previous peak are selected. The pixels in the column around the peak are fitted with a Gaussian function to determine the peak location with a higher accuracy. Taking the derivative of the obtained set of (x,y) points can result in a very noisy profile. To reduce the noise, the points are fitted with a spline function without assuming a particular shape for the set of (x,y) points.

Figure 8 shows the image overlaid with the column peaks (red) and the spline (yellow) fitted through those peaks. Note that the spline is able to jump across the cutouts made by the markers.

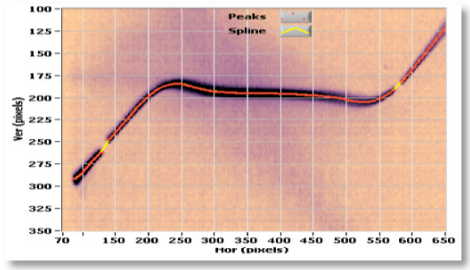

Figure 8: Finding the curve in the image by fitting to the peaks and fitting to a spline.

The fitted spline points can then be fitted to a model-based function to further reduce noise. Fig 9 shows the resulting profiles, the derivatives of the peaks and spline, and a model fitted to the derivative of the spline.

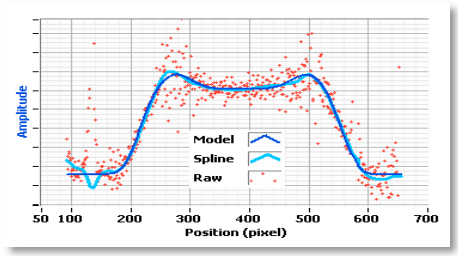

Figure 9: The red points show the derivative of the peaks while the light blue trace shows the derivative of the spline fit. The light blue trace shows a model fit to the spline derivative.

The use of a model-based function also allows us to correct for systematic aberrations. Under certain conditions, a slope appears in the profile. This is seen as a quadratic function in the curve on the fluorescent screen. Calculations have shown, see [3], that if the line scan of the electrons doesn't go exactly through the diagonal center of the quadrupoles, such a deviation can occur. We can add this deviation to the modeling function while fitting and then remove it from the final plot.

A typical model-based function for a particle beam is the Gaussian function. However, in case of the SNS Ring, Gaussian shaped beams are painted next to each other, significantly changing the profile in the ring. In fact, the sum of many overlapping Gaussians can approximate a super-Gaussian function, and this shape fits the beam shape rather well, see [4] and [5].

The flexibility in the order of the exponent allows for adjustments in the steepness of the slopes and the flatness of the peak. The painting scheme combined with the space charge effects can leave the middle of the beam less

populated. To account for that, we use the sum of two super-Gaussians with a slope to account for the deviation:

$$f_{DSG}(x) = a_1 \cdot \exp\left(-\left(\frac{|x-\mu|}{\sigma_1}\right)^{n_1}\right) + a_2 \cdot \exp\left(-\left(\frac{|x-\mu|}{\sigma_2}\right)^{n_2}\right) + sl * x + o$$

where a_1 and a_2 are the amplitudes, μ is the centroid, n_1 and n_2 are the orders, σ_1 and σ_2 are the sigmas, sl is the slope, and o is the offset. By varying the order of the expression in the exponent, the flatness and steepness of the slope are adjusted, thus providing a better fit.

Fig. 10 shows an example of the difference in fitting between Gaussians and super-Gaussians. The blue trace of the double super-Gaussian follows the raw data more closely than the double Gaussians, red trace, for the transverse profile, as measured by a wirescanner.

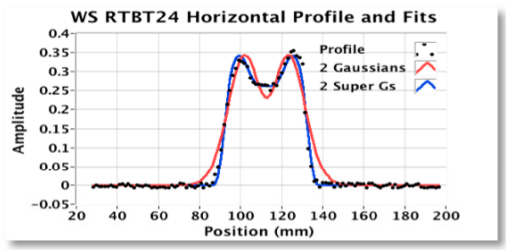

Figure 10: Horizontal profile from a wirescanner.

DATA

The next figures show data obtained with the electron scanner. The data is taken during the December 2010 run. Fig. 11 and Fig. 12 show multiple turns in which each turn is sliced at 25 ns intervals. Turns in between the listed turns are left out. Fig. 13 and Fig. 14 show the improvement the model fit can make to the profiles; noise is reduced and the slope is removed. At higher intensities, above 15 uC, the profiles are not as clean anymore. Part of the curve can project outside of the fluorescent screen. The main limiting factor is that the HV transformer starts arcing around 60-65 kV. Higher accelerating voltages would reduce the amount of deflection, which is needed to keep the electrons on the screen. Additionally, the proton beam slightly defocusses the electron beam, which degrades the obtained profile.

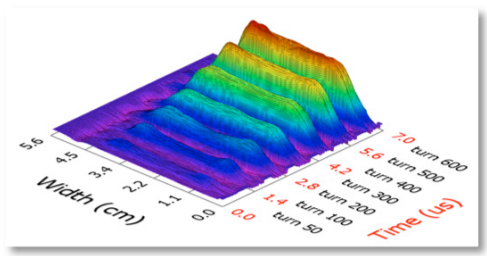

Figure 11: Horizontal profiles from multiple scans through the proton bunch in the same turn.

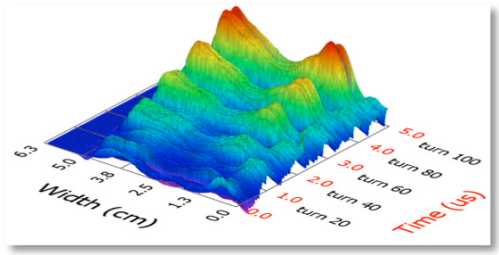

Figure 12: Vertical profiles from multiple scans through the proton bunch in the same turn.

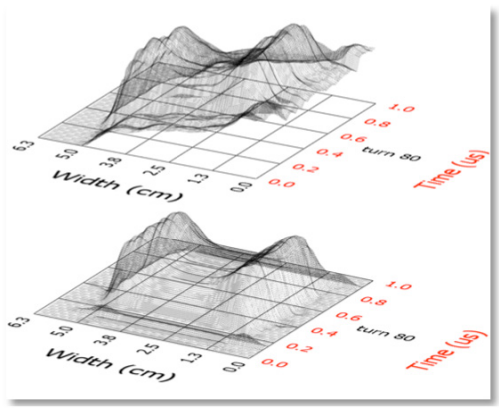

Figure 13: Vertical profile of turn 80 in the ring. The top plot shows the spline results. The bottom plot shows the fitted results with the slope removed.

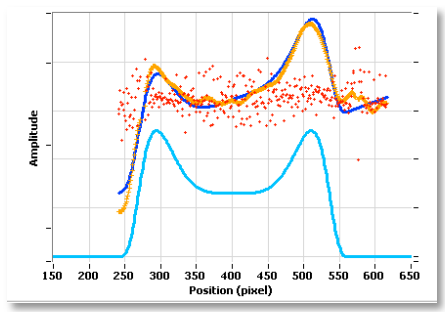

Figure 14: The removal of the slope from the fitted data.

DISCUSSION

We have made several improvements to the electron scanner. We installed more sensitive cameras, improved the timing system [6], added magnetic shielding, and reduced noise in the profile by fitting to the obtained profile [7].

We have further improved the timing jitter from about 10 ns to about 1 ns, by installing a commercial delay generator PXI board.

The orientation of the deflectors was to be exactly 45 degrees but appears in the images to be different for both planes. The horizontal profile size must be decreased by about 20%, while the vertical profile size must be increased by about 20%. Unfortunately, due to lack of technician availability we were not able to confirm our suspicions by inspecting the inside of electron scanner.

The possible alignment error can also mean that the deflectors are not exactly aligned with the quadrupoles and thus explain the curving of the straight line although this deviation is very small for the horizontal profile and can be diminished by aligning the projected curve onto a different location of the screen.

After each production setup, the wire scans are saved and these scans from the last production run in 2010 are used to compare with ES profiles obtained during that run. Using the accelerator model, the wire scanner profiles are scaled to the ring location of the electron scanner. Figure 15 shows these results. The profiles are measured at almost 20 μC of beam charge and are not as clean as the lower intensity profiles but this is the most recent data we have available. The corrections for the off-angle deflectors have been applied. The asymmetry of the ES profiles is surprising and we are not sure to what causes this. If confirmed, we will have to add the asymmetry to the model-based function. The asymmetry has also been observed, at times, in wire scanner profiles. The horizontal profiles match well with FWHM values of 37.8 mm for the ES and 37.6 mm for the wirescanner. The vertical profiles match to about 10 percent, 56.6 mm for the ES and 51.5 mm for the wirescanner. The ES profile doesn't show the full size, the ES aperture is too small. However, the derivative of an image curve taken without beam still gives us the baseline for use in the plot. The amplitudes of the wirescanners are adjusted to match with the electron scanner profiles. The width adjustment for the wirescanner profiles is taken from the model calculations. The error in the model calculations is estimated to be less than 20%.

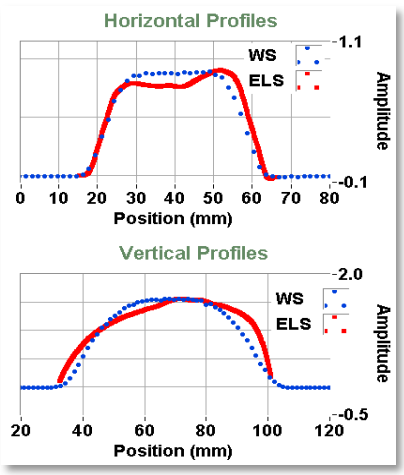

Figure 15: Comparison of profiles.

A beam bump study was done, see [7], to compare the BPM (Beam Position Monitor) measurements with the electrons scanner profiles center positions. Applying the corrections for the deflector angles, the values agree to ~10%, step size of about 10.4 mm vs. 9.4 mm (BPM vs ES) for the horizontal plane and ~20% for the vertical plane 13.0 mm vs. 15.9 mm.

FUTURE

With beam intensities above about 17 μC per bunch, the curve of the electrons no longer fits onto the screen. We hope to upgrade the HV transformer to accelerate the electrons up to 75 kV and thus decrease the deflection. More sensitive cameras would allow us to turn down the electron heating while still seeing the scan. This will help us reduce unintended blobs on the screen that appear related to high heating currents. While the design goal was to keep the deflectors at 45 degrees, we know how to correct the projections. Rotating the deflectors (and quads) to a steeper angle can give us a quick and cheap way to increase the aperture of the electron scanner without having to redo the vacuum chamber.

SUMMARY

The electron scanner provides SNS with the unique capability to view the profiles, both transverse and longitudinal, in the ring throughout most of the accumulation cycle. Software is available to control the electron scanner and direct it to make multiple measurements. We see agreement to about 10% between the electron scanner profiles and the model calculations on the RTBT ((Ring to Target Beam Transferline) wirescanner profiles and to about 20% compared to BPM measurements. We plan to do more studies at the lower intensities to further confirm the accuracy of the electron scanner.

ACKNOWLEDGEMENTS

The authors would like to acknowledge several of the many people who have worked on the electron scanner or helped taking data: T, Pelaia setup the orbit bumps. The work of S. Aleksandrov, D. Malyutin and S. Starostenko, was essential to the implementation of the electron scanner.

REFERENCES

[1] A. Aleksandrov et al, "Feasibility Study of Using an Electron Beam for Profile Measurements in the SNS Accumulator Ring," Proc. PAC 2005, pp. 2586-2588.
[2] E. Tsyganov, et al, "Electron beam emittance monitor for the SSC," Proc. PAC1993, p. 2489-2491.
[3] D.A. Malyutin, "Electrons Outside of Quad Centers", Internal Memo, SNS/RAD, ORNL, Dec 2009.
[4] F.-J. Decker, "Beam Distributions Beyond RMS", 6th Workshop on Beam Instrumentation," Vancouver, Canada, 3 - 6 Oct 1994, p. 550
[5] W. Blokland et al, "Fitting RTBT Beam Profiles: the case for the Super-Gaussian," Internal Memo, SNS/RAD, ORNL, Nov 2009.
[6] W. Blokland et al, "Electron Scanner for SNS Ring Profile Measurements," Proc. DIPAC'09, Basel, Switzerland, May 2009, p. 155-7
[7] W. Blokland, "Non-Invasive Beam Profile Measurements Using An Electron-Beam Scanner," Proc. HB 2010, Morschach, Switzerland, p. 438-442.